Supplemental Information

Table S1 Demographic data

Characteristic	SLE patients(n=11)	Healthy donors(n=19)
Sex (male/female)	2/9	3/16
Age, years (mean±SD)	41.55±14.34	37.53±11.89
Disease duration, months (mean±SD)	60.45±50.14	—
SLEDAI score (mean±SD)	9.46±5.24	—
Anti-ANA（positive/negative）	11/0	—
Lupus nephritis (positive/negative)	7/4	—
Proteinuria (positive/negative)	7/4	—

ANA, antinuclear antibody, *SLE*, Systemic lupus erythematosus, *SLEDAI*, Systemic Lupus Erythematosus Disease Activity Index

www.pnas.org/cgi/doi/10.1073/pnas.1901340116

A

Model	Autoimmune phenotype	Refs.
Pristane (TMPD) induced	Anti-ANA IgG, IgG immune complexes mediated glomerulonephritis, enlarged spleen, lung disease	43-45
B6·H-2^{bm12} → B6 cGVHD	Anti-ANA IgG, IgG immune complexes mediated glomerulonephritis, enlarged spleen	35, 46-47
Ship$^{fl/fl}$CD79a$^{Cre/+}$, Ship$^{fl/fl}$-Aicda$^{Cre/+}$	Anti-ANA IgG, IgG immune complexes mediated glomerulonephritis, enlarged spleen, lung disease	48-50

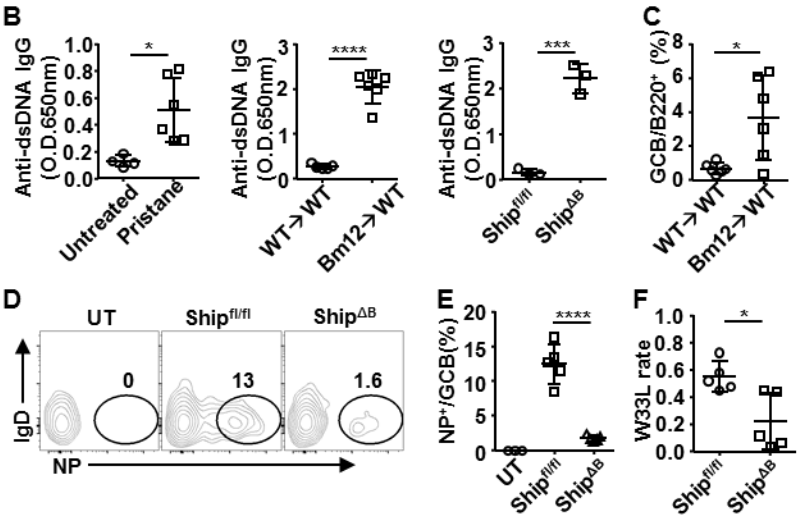

Figure S1. Autoantibody production and impaired antibody affinity maturation in lupus mice. (A) Murine lupus models in this study. (B) Anti-dsDNA IgG autoantibody levels in TMPD-induced mice, Bm12 cGVHD mice, and Ship$^{\Delta B}$ mice. (C) Percentage of GCB cells among total B cells in Bm12 cGVHD lupus mice. (D-E) Representative FACS profile (D) and bar-graph (E) showing the percentage of NP-specific GCB cells in Ship$^{fl/fl}$ and Ship^{flox} mice. (F) W33L rate of splenic V186.2 –Cg1 transcripts in mice in (E). Each symbol in bar-graphs represents an individual mouse. Bars represent mean ± SD. * $p \leqslant 0.05$, *** $p \leqslant 0.001$, **** $p \leqslant 0.0001$; unpaired two-tailed t-test (B, C, F), one-way ANOVA with Sidak's multiple comparisons test (E). A representative of two (C) or three (B, D-F) independent experiments is shown.

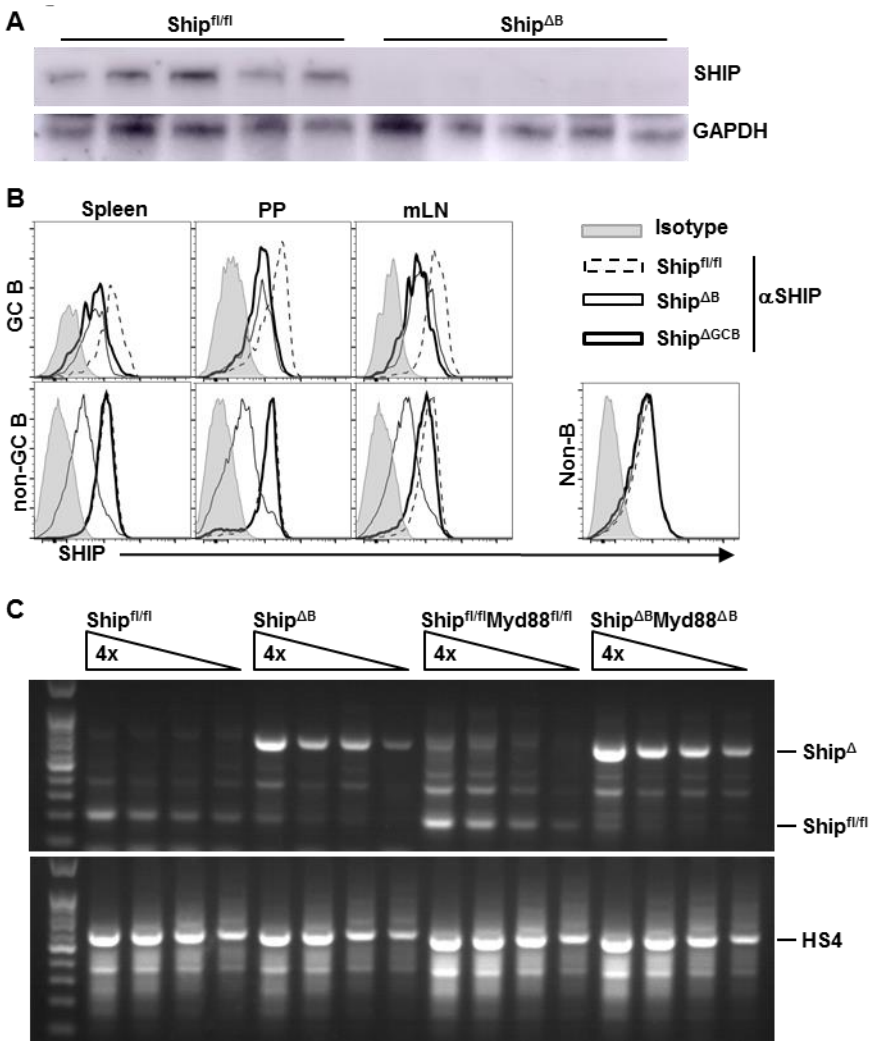

Figure S2. Ship is efficiently deleted in Ship$^{\Delta B}$ B cells and Ship$^{\Delta GCB}$ GCB cells. (A) Ship levels in FOB cells isolated from Ship$^{fl/fl}$ or Ship$^{\Delta B}$ mice, quantified by western blot. (B) Representative FACS profile showing Ship levels in GC or non-GC B cells in the indicated tissues of the indicated mice. (C) Semi-quantitative PCR analysis of indicated Ship alleles in B cells isolated from the indicated mice, with HS4 fragments were PCR amplified as loading controls.

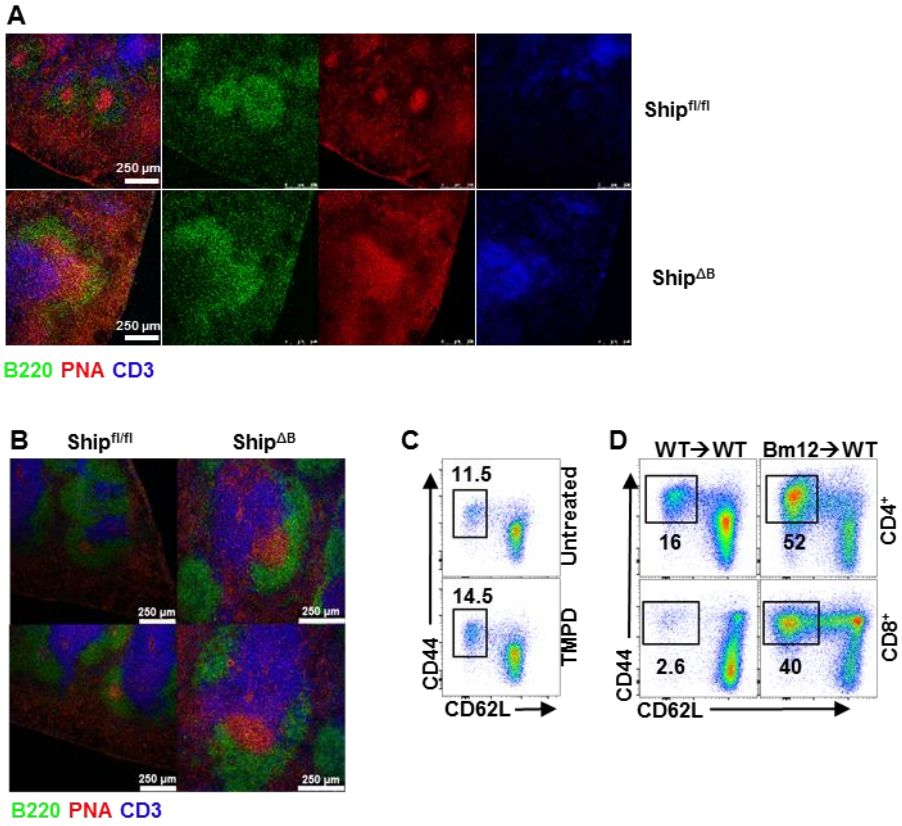

Figure S3. Spontaneous GC and aberrant T cell activation in lupus mice. (A) Immunofluorescence image (single channels) of frozen sections of spleens from $Ship^{fl/fl}$ mice and $Ship^{\Delta B}$ mice analyzed 2 weeks after NP-CGG immunization. (B) Immunofluorescence image of frozen sections of spleens from $Ship^{fl/fl}$ and $Ship^{\Delta B}$ mice. (C-D) Representative FACS profile showing the percentage of $CD44^{+}CD62L^{-}$ effector/memory cells (T_{EM}) among splenic $CD4^{+}$ and $CD8^{+}$ T cells in TMPD-induced lupus mice (C), control or Bm12 cGVHD lupus mice (D). A representative of two (D) or three (B-C) independent experiments is shown.

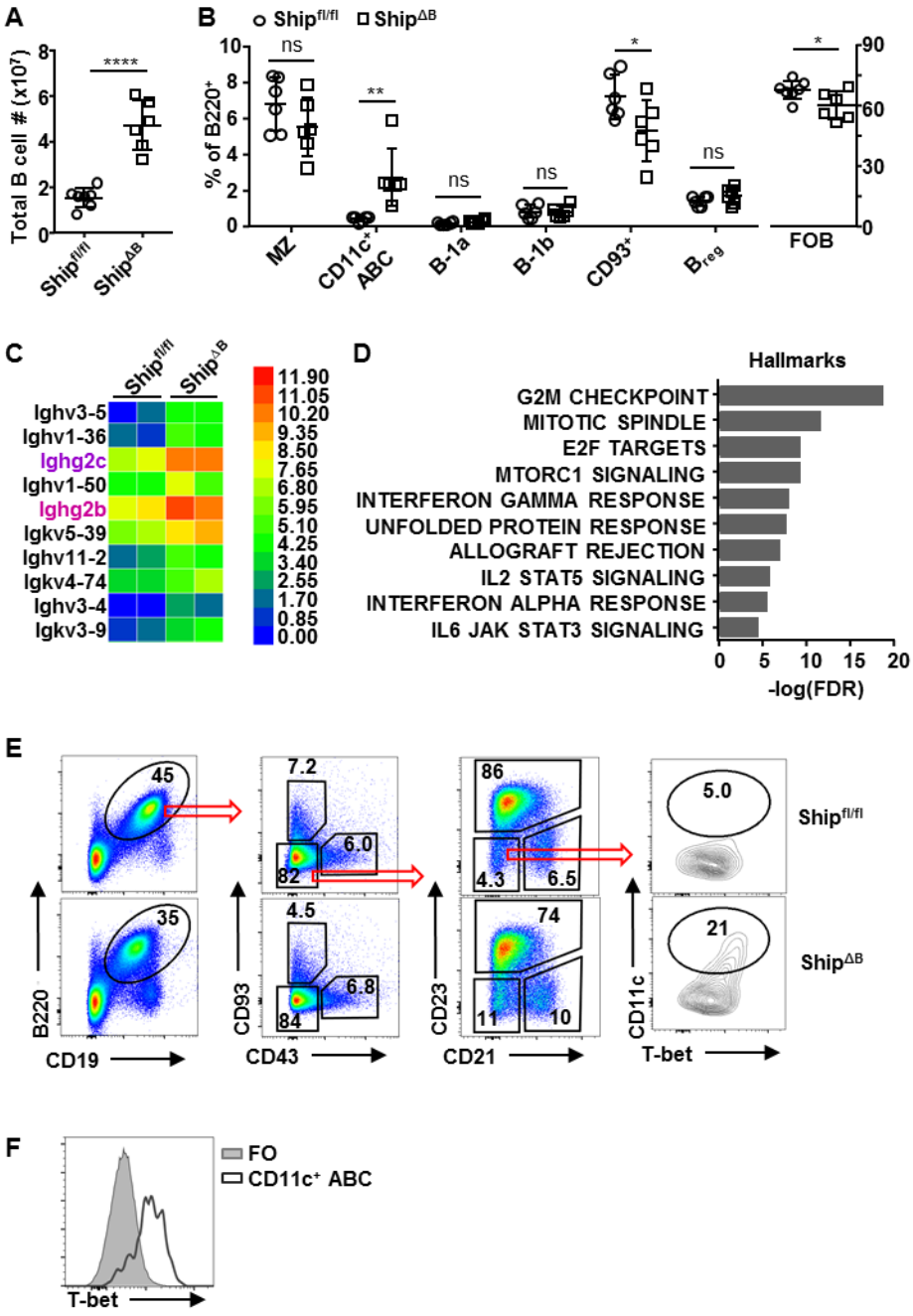

Figure S4. Increased CD11c^{+} ABCs in Ship$^{\Delta B}$ mice. (A, B) Bar-graph showing the absolute cell number of splenic B cells (A) or frequency of follicular B cell (FOB), marginal zone B cell (MZ), B-1a, B-1b, transitional B cell (CD93^{+}), CD11c^{+} ABC and Breg among splenic B cells in Ship$^{fl/fl}$ and Ship$^{\Delta B}$ mice. (C) Heat map showing the log-transformed expression of immunoglobulin genes in B-lineage cells (B220^{+} and B220^{low}CD138^{hi}) sorted by flow cytometry from Ship$^{fl/fl}$ mice and Ship$^{\Delta B}$

mice at the age of 16-20 weeks (n = 2). (D) Top 10 GSEA Hallmark pathways enriched for $Ship^{\Delta B}$ B cells relative to $Ship^{fl/fl}$ B cells, among genes expressed differentially between $Ship^{fl/fl}$ and $Ship^{\Delta B}$ B cells with a p-value less than 0.01. (E) Gating strategy of $CD11c^{+}Tbet^{+}$ ABCs in the spleens of $Ship^{fl/fl}$ and $Ship^{\Delta B}$ mice. (F) Representative FACS profile of Tbet expression in the $CD11c^{+}$ ABCs and FOB cells. Each symbol in bar-graphs represents an individual mouse. Bars represent mean ± SD; ns, not significant, * $p \leqslant 0.05$, ** $p \leqslant 0.01$, **** $p \leqslant 0.0001$; unpaired two-tailed t-test (A, B). A representative of three independent experiments is shown (A, B, E, F).

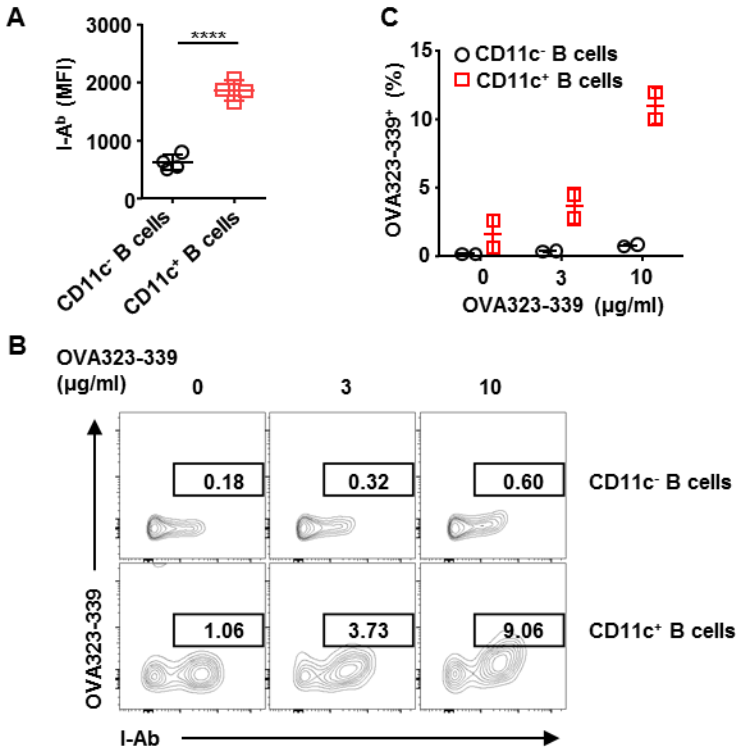

Figure S5. CD11c$^+$ ABCs present more antigens than CD11c$^-$ B cells. (A) Mean fluorescence intensity (MFI) of I-A^b of WT CD11c$^+$ B cells and CD11c$^-$ B cells; (B,C) Representative FACS profile (B) and bar-graph (C) showing the percentage of OVApeptide$^+$ cells among WT CD11c$^+$ B cells and CD11c$^-$ B cells cultured for 18 hours in the presence of the indicated concentrations of OVA peptide. Each symbol in bar-graphs represents an individual or mouse (A) or incubation (C). Bars represent mean ± SD; **** p ⩽0.0001, unpaired two-tailed t test . A representative of three independent experiments is shown (A-C).

Supplemental Methods

Mice

Ship$^{\Delta B}$(*Ship$^{fl/fl}$CD19-Cre^{+}*)(1) and Cγ1-Cre(2) mice were kindly provided by Dr. Jeffrey Ravetch (The Rockefeller University). Myd88$^{fl/fl}$(B6.129P2(SJL)-*Myd88^{tm1Defr}*/J)(3), B1-8^{hi}(B6.129P2-*Ptrpc^{a}Igh^{tm1Mnz}*/J) and B1-8^{low}(B6.129P2-*Igh^{tm2Mnz}*/J)(4), Bm12(B6(C)-*H2-Ab1^{bm12}*/KhEgJ), *TCRβ$^{-/-}$ TCRδ$^{-/-}$*(B6.129P2-*Tcrb^{tm1Mom}Tcrd^{tm1Mom}*/J)(5), μMT(B6.129S2-*Ighm^{tm1Cgn}*/J)(6), and CD11c-DTR (B6.FVB-*1700016L21Rik$^{Tg(Itgax-DTR/EGFP)57Lan}$*/J)(7) mice were purchased from The Jackson Laboratory. Ship$^{\Delta B}$B1-8^{hi}(*Ship$^{fl/fl}$CD19-Cre^{+}*, B1-8^{hi}), Ship$^{\Delta B}$B1-8^{lo}(*Ship$^{fl/fl}$CD19-Cre^{+}*, B1-8^{lo}), and Ship$^{\Delta B}$Myd88$^{\Delta B}$(*Ship$^{fl/fl}$Myd88$^{fl/fl}$CD19-Cre^{+}*) mice were generated by crossing Ship$^{\Delta B}$ mice with B1-8^{hi}, B1-8^{hi}, and Myd88$^{fl/fl}$ mice, respectively. WT C57/BL6 mice were purchased from Shanghai SLAC Laboratory Animal Company. All mice were maintained in the specific-pathogen-free (SPF) animal facility at Shanghai Jiao Tong University School of Medicine (SJTUSM). All animal experiments were performed in compliance with institutional guidelines and had been approved by SJTUSM Institutional Animal Care and Use Committee.

FACS (Flow cytometry)

FACS analyses were performed using BD LSRFortessa™ X-20 analyzer (BD Biosciences) or BD FACSCanto II (BD Biosciences). Mouse cells were stained with anti-B220 (RA3-6B2), CD38 (90), GL7 (GL7), IgD (11-26c) and NP-PE (Biosearch Technologies) for NP-specific GC B cell analysis, with anti-B220, CD38, CD95 (Jo2), CD45.1 (A20), CD45.2 (104) for B1-8^{hi} cell expansion analysis, with anti-CD4 (RM4-5), CD8a (53-6.7), CD44 (IM7), CD62L (MEL-14) or with anti-CD4, CD8, PD-1 (J43), CXCR5 (2G8) for T_{EM} cell or T_{FH} cell analysis. For Ship-expression assay, cells were stained with anti-B220, CD38, GL7, Ship-1 or the isotype control antibody. Human PBMCs were isolated using Lymphoprep™ (STEMCELL) and stained with anti-CD19(HIB19), IgD(IA6-2), CD21(1048), CD27(O323) and CD11c (Bu15) for CD11c^{+} ABC analysis, with anti-CD4(RPA-T4),

CD45RA(HI100), CXCR5(RF8B2), PD-1(EH12.1) and ICOS(C398.4A) for T_{FH} analysis. Intracellular staining of Tbet was performed using eBioscience™ Foxp3/Transcription Factor Staining Buffer Set (Thermo Fisher) and anti-Tbet antibodies (4B10; Biolegend). For phospho-flow analysis, stimulated splenocytes were fixed with 2% polyformaldehyde, permeabilized with Perm/Wash buffer (BD), and stained with anti-ERK or anti-pERK antibodies (CST). All antibodies were purchased from BD Biosciences, Biolegend or eBiosciences.

B cell purification

Follicular B cells were magnetically (MACS) sorted. Splenocytes were incubated in MACS buffer (PBS, pH 7.2, 0.5% BSA, 2 mM EDTA) with biotinylated anti-CD43(2.5 μg/ml), anti-CD11c (2 μg/ml) and anti-GL7(2 μg/ml) for 25 min, washed with MACS buffer, then incubated with anti-biotin microbeads (Miltenyi) for 20 min. After washing with MACS buffer, cells were loaded on the LS column (Miltenyi), and the flow-through was collected as follicular B cells. Pan-B cells were isolated with a B cell Isolation Kit (Miltenyi), followed by another round of sorting using biotinylated anti-CD11c or anti-CD11c plus anti-GL7 to generate CD11c- B cells and FO B cells, respectively.

$CD11c^+$ ABC differentiation and T cell activation

MACS-sorted follicular B cells (see above) were cultured in the presence of 1 μg/ml CL097 (Invivogen), 25 ng/ml IL-21(Peprotech) or their combination for 36~84 hours before FACS analysis. MACS-sorted OT-II pan-T cells (Miltenyi, 130-095-130) were labeled with CFSE (Invitrogen) and co-cultured with various MACS-sorted B cells (see above) in the presence of 0.3 or 1 μg/ml $OVA^{323-339}$ peptide (Genescript) for 36-84h before analysis of T cell activation/proliferation by FACS.

Autoantibodies

Anti-nuclear and anti-dsDNA IgG antibodies were detected by ELISA (Demeditec, DE7020 and QUANTA Lite, 708510). $Ship^{\Delta B}$ splenic follicular B cells ($B220^{+}CD19^{+}CD43^{-}CD93^{-}CD23^{+}$) and $CD11c^{+}$ABCs ($B220^{+}CD19^{+}CD43^{-}CD93^{-}CD23^{-}CD21^{-}CD11c^{+}$) were FACS-sorted (>95% pure) and co-cultured with NB-21.2D9 feeder cells as described (8) and analyzed 10 days later for total IgG and anti-dsDNA IgG levels with ELISA.

RNA-Seq

RNA-Seq used FACS-sorted WT and $Ship^{\Delta B}$ splenic pan-B cells ($CD19^{+}$ and $CD19^{lo}CD138^{hi}$, purity > 95%). Paired-end reads (~ 20 million/sample) was aligned to the mouse reference genome (mm10) using Tophat2. Gene expression counts were quantified by HTSeq. Differential expression analysis was performed using R package DESeq2. *P*-values obtained from multiple tests were adjusted using Benjamini-Hochberg correction. The Molecular Signatures DataBase v 6.2 (Broad Institute) was used as a source of gene sets with defined functional relevance. Nominal P values were FDR corrected, and gene sets with an FDR of < 0.05 (the top 10 values of -logFDR) were used for Gene Set Enrichment Analysis (http://www.broad.mit.edu/gsea/index.html). Data were deposited at NCBI-SRA (accession number: PRJNA523485).

Immunofluorescence

Eight-μm frozen sections were probed with antibodies against B220-Alexa Fluor 488 (RA3-6B2; Biolegend), CD3-Alexa Fluor 647(17A2; Biolegend) and Biotinylated peanut agglutinin (PNA) (Vector), followed by staining with PE-conjugated streptavidin. Slides were viewed and photographed with a Leica TCS SP8 confocal microscope.

Western blot

Follicular B cells (see above) stimulated with CL097, αIgM $(Fab)_2$' or intact anti-IgM(Jackson ImmunoResearch) were lysed with RIPA buffer (with 1mM PMSF, ROCHE proteinase inhibitor

cocktail and ROCHE phosSTOP). Protein samples were separated by 10% SDS-PAGE gel and blotted to a 0.45 μm PVDF membrane (Millipore). Membranes were probed with the targeting antibodies and then visualized using Chemiluminescent GRP substrate (Millipore).

In vitro test of antigen presentation

C57BL6/J splenocytes were isolated and cultured in RPMI medium with 10% FBS (HyClone), 2 mM glutamine, 5 mg/ml sodium pyruvate, 20 U/ml insulin, 1% non-essential amino acids, 50 μM 2-ME, in the presence of 0, 3 or 10 μg/ml n-biotinylated OVA peptide (323-339) (ChinaPeptides, Shanghai). Cells were incubated at 37°C and 5% CO2 for 18 hours before flow cytometry analysis.

Statistical analysis

Data were analyzed with Prism GraphPad 6.0.

References

1. Leung WH*, et al.* (2013) Aberrant antibody affinity selection in SHIP-deficient B cells. *European journal of immunology* 43(2):371-381.
2. Casola S*, et al.* (2006) Tracking germinal center B cells expressing germ-line immunoglobulin gamma1 transcripts by conditional gene targeting. *Proceedings of the National Academy of Sciences of the United States of America* 103(19):7396-7401.
3. Hou B, Reizis B, & DeFranco AL (2008) Toll-like receptors activate innate and adaptive immunity by using dendritic cell-intrinsic and -extrinsic mechanisms. *Immunity* 29(2):272-282.
4. Shih TA, Roederer M, & Nussenzweig MC (2002) Role of antigen receptor affinity in T cell-independent antibody responses in vivo. *Nature immunology* 3(4):399-406.
5. Mombaerts P*, et al.* (1992) Mutations in T-cell antigen receptor genes alpha and beta block thymocyte development at different stages. *Nature* 360(6401):225-231.

6. Kitamura D, Roes J, Kuhn R, & Rajewsky K (1991) A B cell-deficient mouse by targeted disruption of the membrane exon of the immunoglobulin mu chain gene. *Nature* 350(6317):423-426.
7. Jung S*, et al.* (2002) In vivo depletion of CD11c+ dendritic cells abrogates priming of CD8+ T cells by exogenous cell-associated antigens. *Immunity* 17(2):211-220.
8. Kuraoka M*, et al.* (2016) Complex Antigens Drive Permissive Clonal Selection in Germinal Centers. *Immunity* 44(3):542-552.